Geochronology of Eocene plutonism and metamorphism in northest Turkey: evidence for a possible magmatic arc

Aral Okay [a] and Muharrem Satır [b]

[a] *Avrasya Yerbilimleri Enstitüsü, İstanbul Teknik Üniversitesi, Ayazağa 34469 Istanbul, Turkey,*
[b] *Institut für Geowissenschaften, Universität Tübingen, Wilhelmstraße 56, D-72074 Tübingen, Germany,*

Abstract

In northwest Turkey Eocene calc-alkaline intrusions with isotopic ages of 53 Ma to 35 Ma form a WNW-ESE trending belt, ~400 km long and ~60 km wide. In the east, the plutons intrude blueschists representing a subducted passive continental margin sequence with Late Cretaceous (~80 Ma) metamorphic ages. In the vicinity of one of these granitoids a low pressure - high temperature metamorphism has resulted in complete transformation of the blueschist metapelites into andalusite micaschists. The andalusite + cordierite + biotite + muscovite + quartz + K-feldspar + plagioclase paragenesis in the micaschists indicates a pressure of 2 ± 1 kbar and a temperature of 575 ± 50° C during the metamorphism. Rb-Sr muscovite and biotite ages of a micaschist sample are 46 ± 3 and 39 ± 1 Ma, respectively, similar to the 45.0 ± 0.2 Ma U-Pb zircon and Rb-Sr biotite ages from the neighbouring pluton. Development of folds and a new foliation in the andalusite micaschists suggest regional rather than contact metamorphism. The Eocene granitic magmatism and associated LP/HT metamorphism in northwest Turkey have probably formed above a NE directed subduction zone located along the Vardar suture.

© 2006 Lavoisier SAS. All rights reserved

Keywords: LP/HT metamorphism, Eocene magmatism, Turkey, blueschist, granitoid

1. Introduction

The Alpide orogeny in Turkey is the result of the convergence and progressive collision of the Pontide and the Anatolide-Tauride blocks starting in the mid Cretaceous [e.g., 1, 2]. During the convergence and collision, the Anatolide-Tauride Block, which formed the passive margin, underwent regional metamorphism and associated penetrative deformation. The regional metamorphism in the Anatolide-Tauride Block shows a general southward younging from mid-Cretaceous in the Tavşanlı Zone [3] to Eocene in the Menderes Massif [4-6] (Fig. 1). This is accompanied by the southward progression of contractional deformation from mid-Cretaceous penetrative ductile deformation on the northern margin of the Anatolide-Tauride Block to Miocene thrusting in the Lycian Taurus [7]. Here, we report an anomaly in this picture, an Eocene magmatic and low pressure - high temperature (LP/HT) metamorphic event, on the northern margin of the Anatolide-Tauride Block, which locally overprints the Cretaceous HP/LT metamorphic rocks. We discuss two possible causes of this Eocene thermal anomaly: oceanic subduction and slab break-off.

2. Tectonic setting

In northwest Turkey the northern margin of the Anatolide-Tauride Block is defined by the İzmir-Ankara suture, which forms a profound stratigraphic, metamorphic, and magmatic boundary. To the north of the İzmir-Ankara suture lies the Sakarya Zone of the Pontides, and to the south the Tavşanlı Zone of the Anatolide-Tauride Block (Fig. 1). The tectonostratigraphic units in these zones are shown in figure 2, and are briefly outlined below.

---

* Corresponding author.
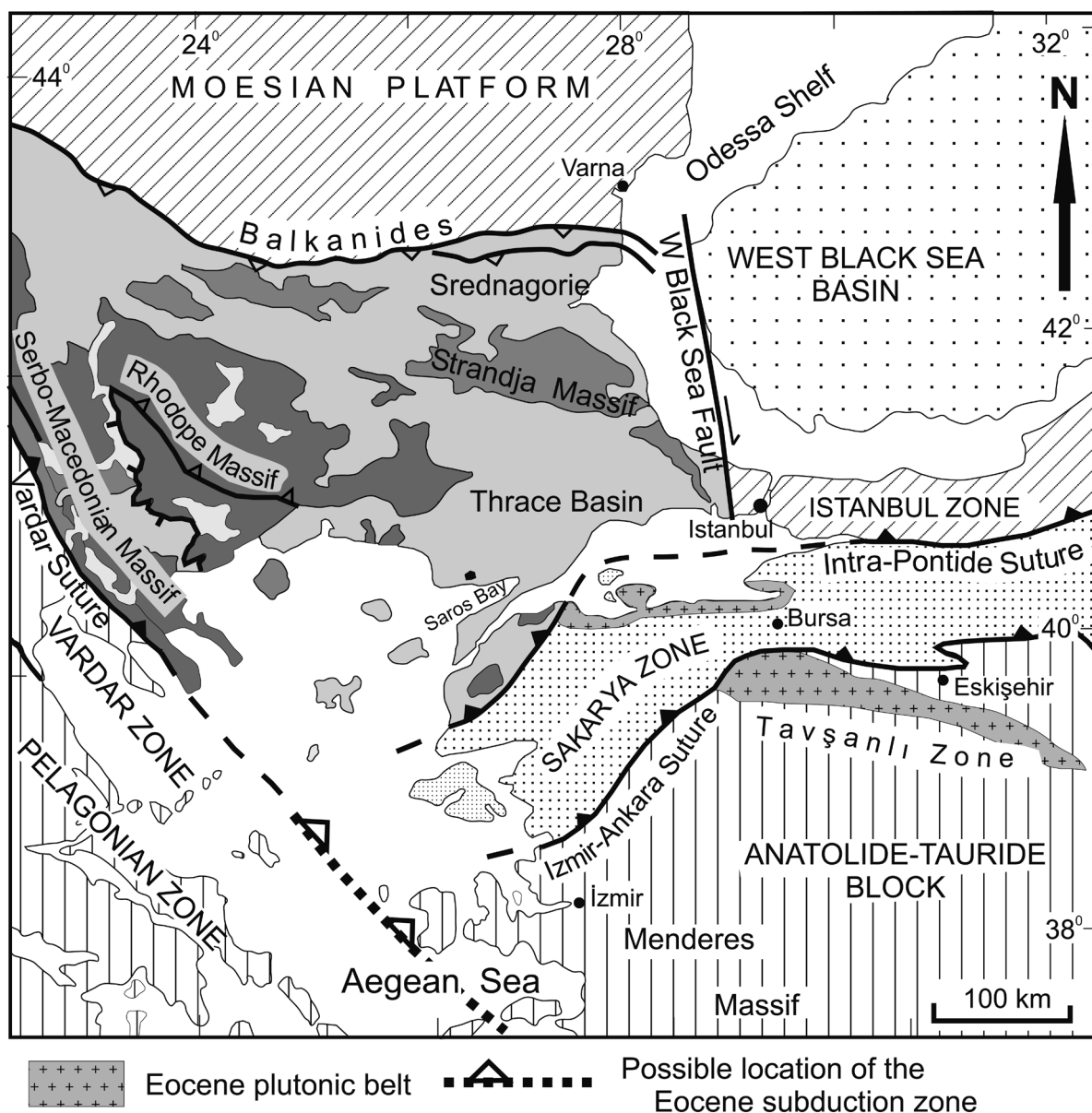*E-mail address:* okay@itu.edu.tr - satir@uni-tuebingen.de

Figure 1: Tectonic map of the northeastern Aegean region. Modified from [65].

2.1. Sakarya Zone

The basement of the Sakarya Zone is made up of high-grade Hercynian metamorphic rocks, which crop out in the Uludağ [8] and Kazdağ [9, 10] mountain ranges (Fig. 2 and 3). They are tectonically overlain by Triassic orogenic series called as the Karakaya Complex [11]. The Karakaya Complex consists of a lower metamorphic series of intercalated Triassic metabasite, marble and phyllite metamorphosed in green-schist and blueschist facies [11, 12]. This Triassic series, named the Nilüfer Formation, is in turn overlain by strongly deformed Permo-Triassic clastic and volcanic rocks of the Upper Karakaya Complex [11, 13]. The Nilüfer Formation and the Upper Karakaya Complex are interpreted as the subduction-accretion units of the Palaeo-Tethys, accreted to the northern margin of Laurasia in the latest Triassic [14-16].

These Cimmerian units are unconformably overlain by the Lower to Middle Jurassic continental to shallow marine clastic rocks and Upper Jurassic-Lower Cretaceous neritic limestones [17] (Fig. 2). Eocene granitoids intrude the Nilüfer Formation in the Kapıdağ peninsula north of Bandırma (Fig. 3).

2.2. The Tavşanlı Zone

The lowermost units exposed south of the suture is a coherent blueschist sequence of probable Palaeozoic-Mesozoic depositional age, and Late Cretaceous (~ 80 Ma) metamorphic age [3, 18]. The blueschist sequence consist of probable Palaeozoic metacla-stic rocks at the base overlain by Mesozoic marble, metabasite, metachert. It is tectonically overlain by a Cretaceous accretionary complex of basalt, radiolarian chert, pelagic shale and pelagic limestone (Fig. 2). The accretionary complex has a melange like
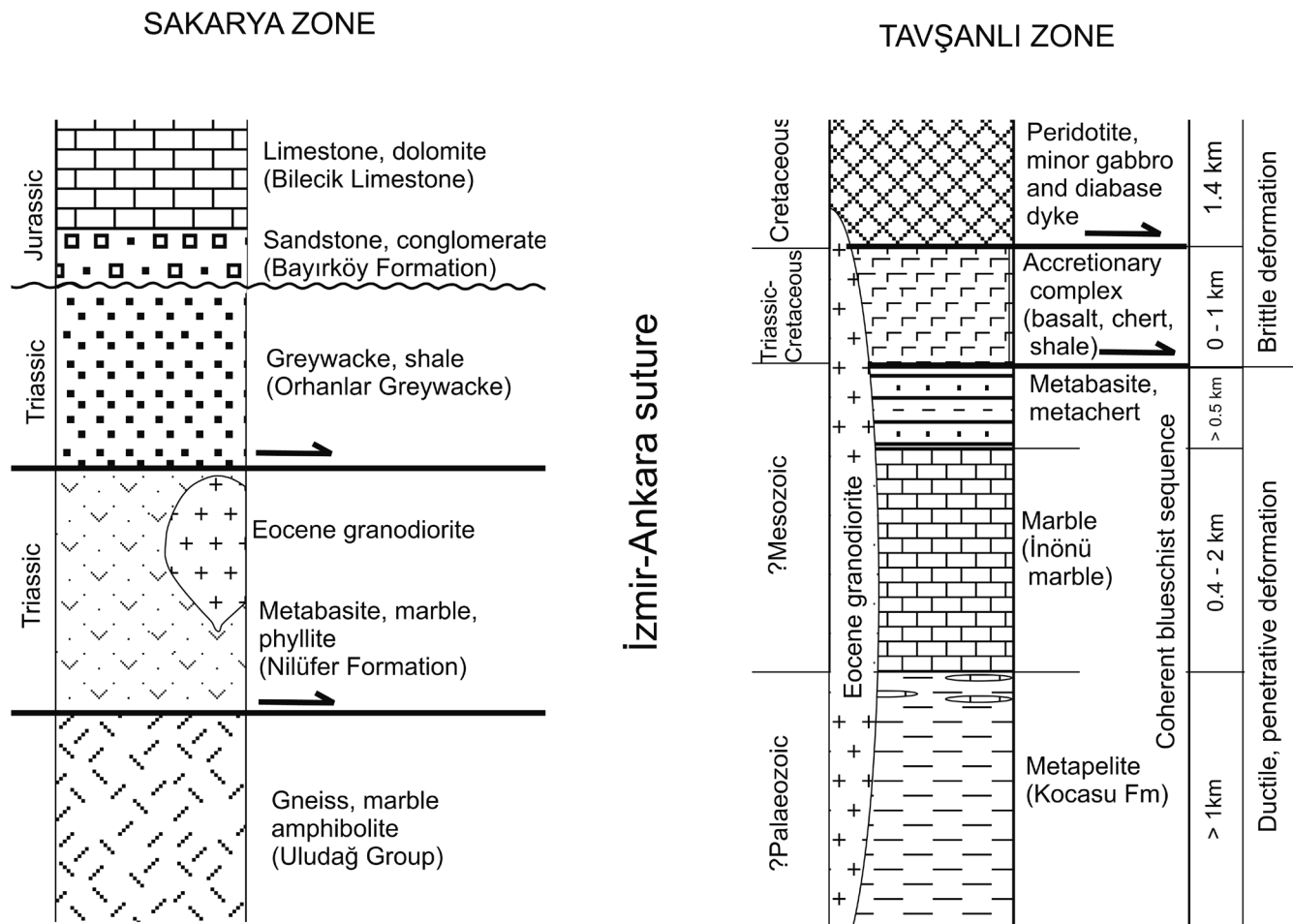
SAKARYA ZONE

TAVŞANLI ZONE

Figure 2: Tectonostratigraphic columns for the Sakarya and Tavşanlı zones in northwest Turkey. Compiled from [2, 18].

incoherent internal structure with large number of faults and shear zones juxtaposing different lithologies. Slices and blocks of radiolarian chert in similar accretionary complexes farther east give ages ranging from Triassic to Cretaceous [21]. The accretionary complex shows an incipient HP/LT metamorphism with local growth of lawsonite, aragonite and sodic pyroxene in the basic volcanic rocks [18].

The accretionary complex and the coherent blueschist sequence are in turn tectonically overlain by large slabs of ophiolite. The ophiolites in northwest Turkey consist mainly of peridotite (more than 90 % of the ophiolite outcrops) with minor gabbro, and are cut by diabase dykes [e.g., 19, 20, 22]. Upper parts of an ophiolite sequence are not recognized. Several post-tectonic granitoid plutons of Eocene age intrude the blueschist sequence, the overlying accretionary complex and the ophiolite [23].

3. Geology of the Eocene plutonism and metamorphism south of Bursa

The area studied lies south of Bursa on the southeastern extension of the Uludağ mountain range. Tectonically it is located immediately south of the İzmir-Ankara suture and largely within the Tavşanlı Zone (Fig. 3 and 4). The lowest

exposed unit in the area is a grey, finely banded, hard, medium grained schist sequence, termed greyschists, which crops out between the towns of Orhaneli and Keles and farther east. The greyschists, over 800 m in thickness, show a strong ductile deformation with the generation of penetrative foliation, lineation and isoclinal folding. The foliation, although highly scattered in strike and dip, is on average subhorizontal. Isoclinal folds in the schists range in amplitude from a few milimetres to several hundred metres. Their axis are subparallel to the mineral streching lineation defined by sodic amphibole and chloritoid with a general east-west trend. Rare metabasite layers are found in the upper parts of the greyschist sequence. The greyschists are overlain by a white marble sequence, with a minimum thickness of 400 m. Near the marble contact, the greyschists are interfolded with small marble and calc-schist lenses. Calcite in the marbles locally shows a strong mineral lineation subparallel to those in the underlying greyschists. The interfolded contacts between marble and schist, the coherence of structures between the two units, marble lenses in schists near the marble contact suggest that the marble has undergone the same deformation and metamorphism as the underlying schist sequence.

The greyschists and the marbles are tectonically overlain by ophiolite, which consists of steeply dipping bands of harz-
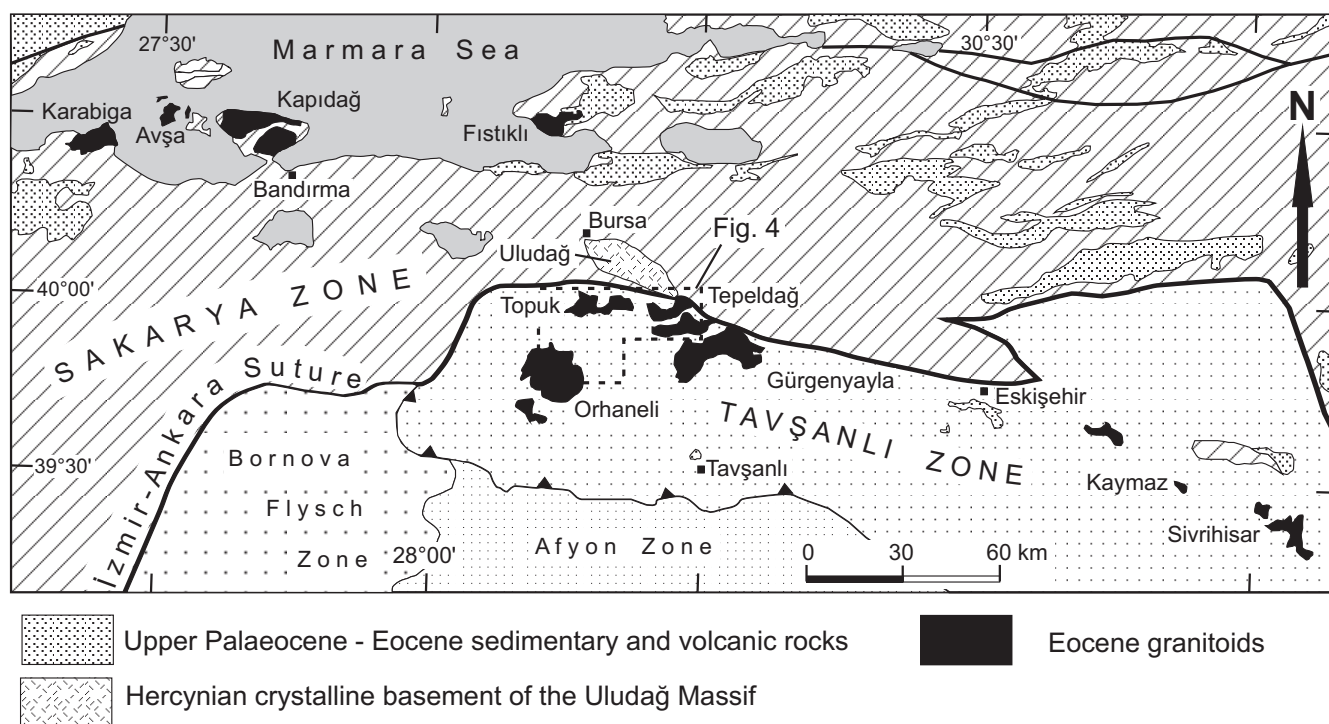
Figure 3: Tectonic map of northwest Turkey, showing the distribution of the Eocene plutons and Eocene sedimentary and volcanic rocks. For location see Fig. 1. Compiled and simplified from [66, 67].

burgite, dunite, clinopyroxenite and gabbro, several kilometres in thickness [19]. Like, elsewhere in western Turkey, the upper extrusive part of the ophiolite sequence is not found. The shallow to medium dip of the basal tectonic contact of the ophiolite, and local gravity surveys indicate a maximum vertical thickness of about 1.5 km for the ophiolite [19]. The ophiolite is intruded by east-west trending diabase dykes.

In the Orhaneli-Keles area post-tectonic calc-alkaline granitoid plutons intrude the blueschist sequence as well as the overlying ophiolite. The Ar-Ar and Rb-Sr biotite and hornblende ages of these plutons are given in table I. The plutons range in age from 53 Ma down to 45 Ma (Early to Mid Eocene) giving a duration of 9 My for the calc-alkaline plutonism [23-25]. No extrusive or hypabysal magmatic rocks of Eocene age are reported from the Tavşanlı Zone. The Eocene plutons are generally homogeneous in texture, grain size and

mineral assemblage and consist of plagioclase + quartz + biotite + K-feldspar + hornblende with ilmenite and sphene as common accessories. Geochemically the Orhaneli and Topuk plutons have a uniform metaaluminous, calc-alkaline compositions compatible with a subduction zone origin [23]. Their trace element geochemistry indicate derivation either from mantle-derived magmas by fractional crystallisation in shallow magma chambers, or from anatexis of crustal lithologies of intermediate composition at pressures less than 10 kbar [23]. Even in the latter case, mantle derived magmas are necessary to induce crustal melting.

The Orhaneli pluton has intruded into the blueschist sequence with the generation of a well-marked hornfels contact metamorphic aureole, about 700 m wide. The quartz + biotite + K-feldspar + plagioclase + cordierite + andalusite assemblage in the inner contact aureole indicates a pressure of 3 ± 1 kbar [23].

The Topuk granitoid intrudes the schist-marble sequence as well as the overlying ophiolite, thus sealing this major tectonic contact. Andalusite and sillimanite are described from the contact metamorphic aureole of the Topuk pluton [19] showing that the Topuk pluton has intruded at a similar depth as the Orhaneli granitoid. The Topuk pluton has also intruded very close and parallel to the suture fault, while staying within the lithologies of the Tavşanlı Zone (Fig. 3 and 4). The suture fault north

Table I: Isotopic ages of the Eocene granitoids from the Tavşanlı Zone.

	Orhaneli	Topuk	Tepeldağ	Gürgenyayla	Sivrihisar
Ar-Ar biotite	52.6 ± 0.4[1]				
	52.4 ± 1.4[1*]				
Ar-Ar hornblende		47.8 ± 0.4[1]			53.0 ± 3.0[5]
Rb-Sr biotite	48.5[2]		44.7 ± 0.4[3]	45.0[4]	
	50.0[2]			45.0[4]	
U-Pb zircon			44.99 ± 0.23[3]		

[1] Harris *et al*. (1994), [2] Ataman (1972), [3] this study, [4] Ataman (1973), [5] Sherlock *et al*. (1999), [1*] from the contact aureole.
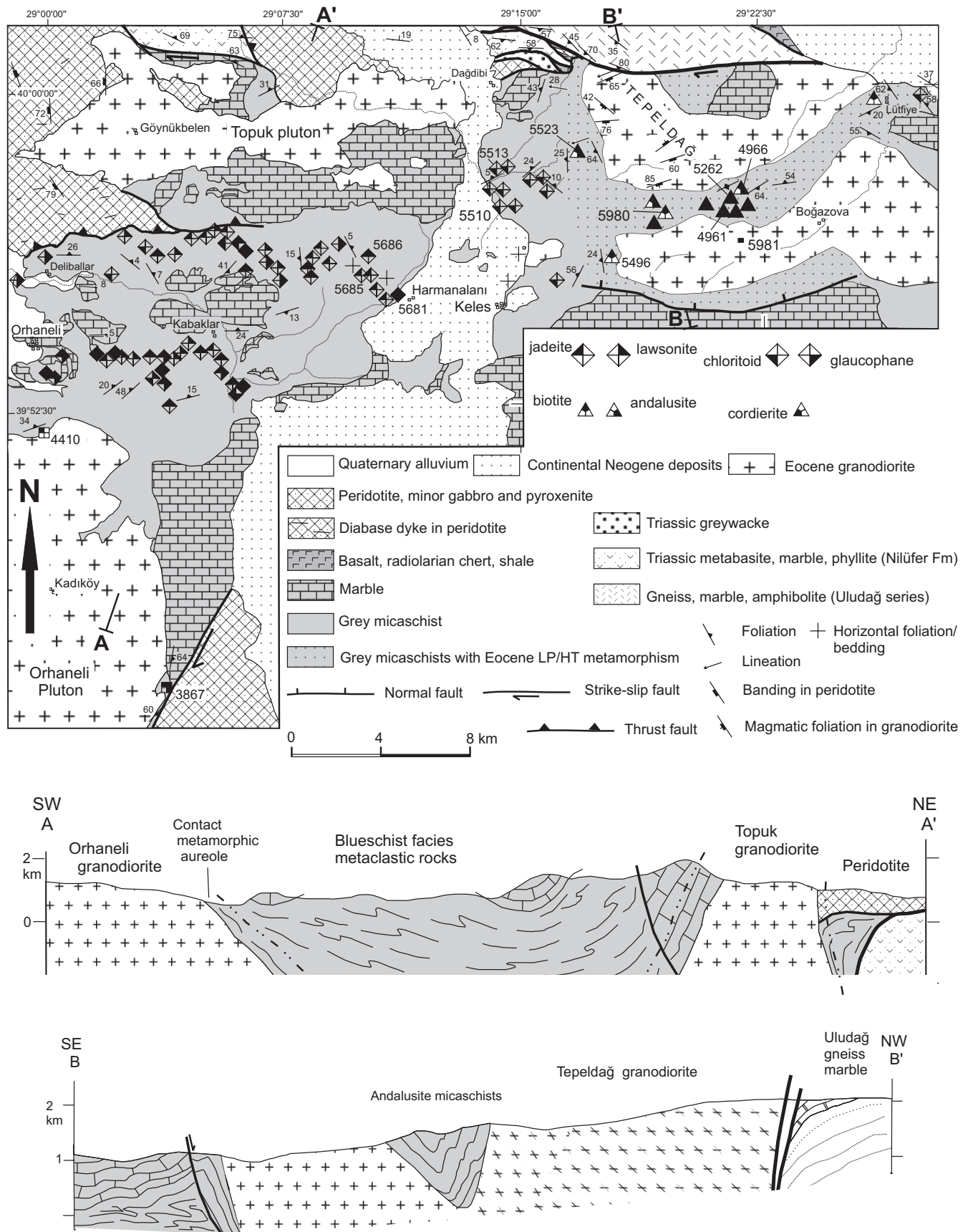
Figure 4. Geological map and cross-sections of the Orhaneli-Keles region with the specimen localities. Based on our mapping and on [19, 68]. For location see figure 3.
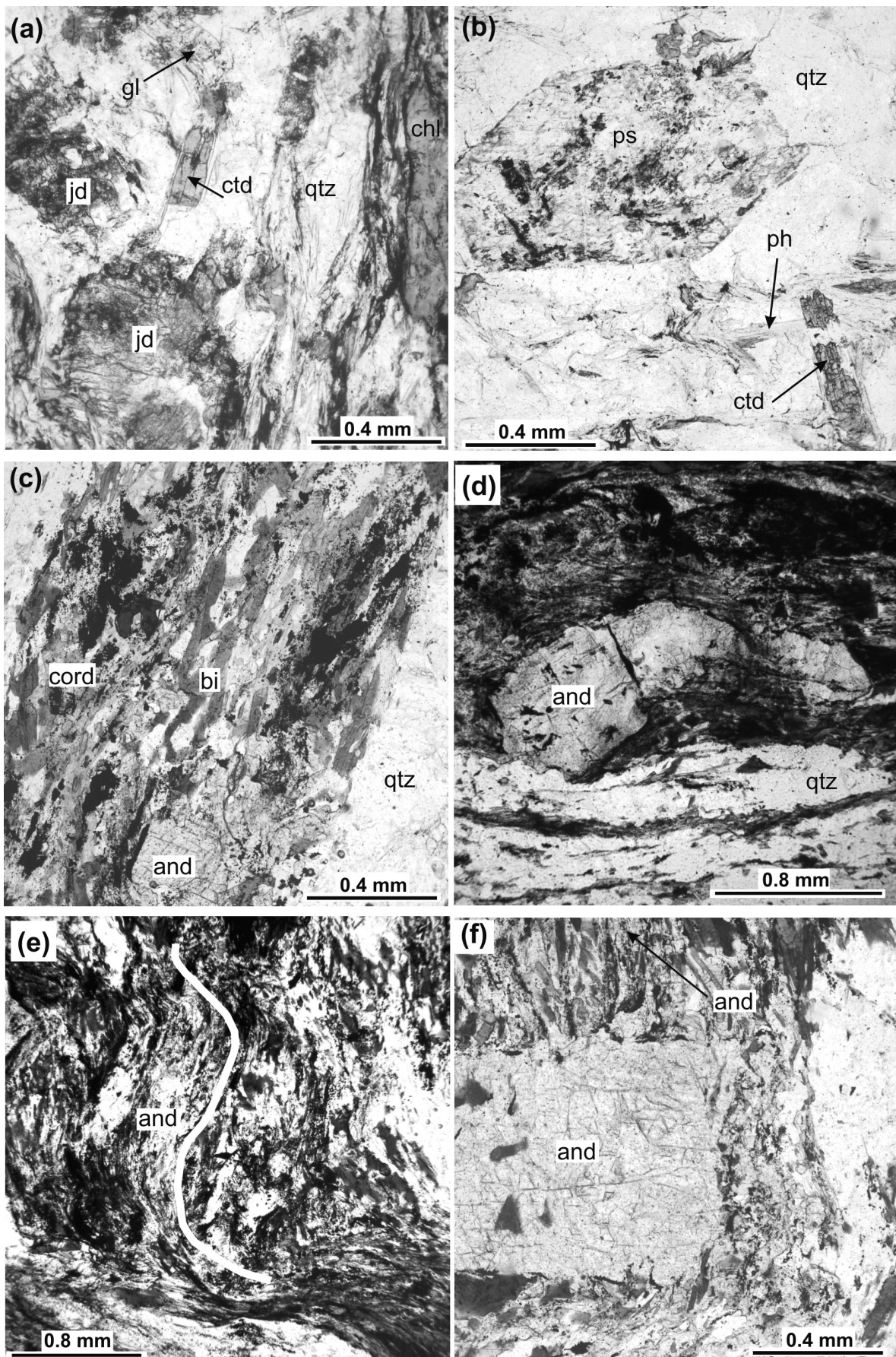
Table II: Estimated modal amounts of the metapelitic samples from the Uludağ region.

	5681A	5685	5686	5510C	5513	5496A	5523	5980	4961	4966	5262
Quartz	43	48	46	35	63	33	31	49	35	40	32
White mica	15	18	19	37	12	19	15	2	3	4	3
Jadeite	20	21	23	-	-	-	-	-	-	-	-
Chloritoid	5	-	-	6	7	-	-	-	-	-	-
Na-amphibole	6	-	-	-	-	-	-	-	-	-	-
Lawsonite	-	-	2	-	-	-	-	-	-	-	-
Garnet	-	-	-	-	-	-	-	-	-	-	-
Plagioclase	-	6	5	4	9	19	17	17	13	11	11
Chlorite	10	6	5	15	8	21	-	-	-	-	-
Biotite	-	-	-	-	-	6	35	21	18	19	32
Andalusite	-	-	-	-	-	-	1	-	11	18	12
Cordierite	-	-	-	-	-	-	-	-	6	-	-
K-feldspar	-	-	-	-	-	-	-	6	9	6	4
Graphite	1	-	-	2	1	1	-	3	2	tr.	3
Opaque	-	1	tr.	1_{py}	$tr._{py}$	$1_{py,ilm}$	$1_{pyr,ilm}$	2_{ilm}	3_{ilm}	2_{ilm}	3_{ilm}
Others		ru			ru		ap		tour	tour	tour

tr.< 0.5; **py**, pyrite; **ilm**, ilmenite; **ru**, rutile; **ap**, apatit; **tour**, tourmaline.

of the Göynükbelen is defined by a steeply-dipping melange belt, a few hundred metres wide, made up of tectonic lenses of serpentinite, basalt, chert, shale, metabasite and marble, which are cut by the undeformed Topuk granitoid. The contact relations, as well as the east-west elongate elliptical shape of the Topuk granitoid, indicate that by the Mid Eocene the suture fault was active and controlled the emplacement of the Topuk pluton.

The Tepeldağ pluton is the least studied of the three Eocene plutons south of Bursa. It is a hornblende-biotite bearing granodiorite to monzodiorite petrographically similar to the Orhaneli and Topuk plutons. The Tepeldağ pluton consists of two bodies about 15 km long, which are connected at a few kilometres depth (Fig. 4). In contrast to the other plutons, the northern Tepeldağ pluton shows locally a steeply dipping and ENE-WSW striking magmatic foliation, mainly defined by

Figure 5: Photomicrographs, plane polarized light. **a.** Greyschist (5681A) with jadeite (jd), chloritoid (ctd), glaucophane (gl), quartz (qtz) and chlorite (chl), **b.** Greyschist (5510C) with chlorite + albite + sericite pseudomorphs (ps) after glaucophane, chloritoid (ctd), phengite (ph) and quartz (qtz), **c.** Andalusite micaschist (5262) with pinitised cordierite (cord), andalusite (and), biotite (bi), graphite and quartz (qtz), **d.** A bend andalusite porphyroblast (and) in the micaschist (sample 5259), **e.** A strongly poikilitic andalusite porphyroblast (and) with spiral shaped graphite and biotite inclusion trails (sample 5264), **f.** Andalusite stringers attached and in optical continuity with the andalusite porphyroblast (and) but growing into the foliation plane (sample 5262). Microstructures shown in Figs. 5d, e and f indicate the regional rather than contact metamorphic character of the andalusite micaschists.

the hornblende crystals, and flattened xenoliths. In the north, the subvertical suture fault juxtaposes the Uludağ gneiss and marble with the Tepeldağ granitoid. Near the suture fault a tectonic foliation, defined by the recrystallisation of quartz into ribbons, has developed in the granitoid.

The Uludağ Group made up of gneiss and marble, and the Nilüfer formation of metabasite, phyllite and recrystallized limestone crop out north of the suture fault (Fig. 4). There are also narrow slivers made up of Triassic greywacke within the suture zone.

4. Petrology and P-T conditions

Greyschists between the towns of Orhaneli and Keles are characterized by the presence of high pressure metamorphic minerals jadeite, lawsonite and sodic amphibole (Fig. 4) [26]. The common mineral assemblage in the greyschists in this region is quartz + white mica ± jadeite ± chloritoid ± glaucophane ± lawsonite ± chlorite. The rare metabasites in the upper parts of the greyschist sequence have the paragenesis glaucophane + lawsonite + phengite + chlorite ± sodic pyroxene ± garnet These rocks are described in detail in Okay and Kelley [27] and Okay [26]. Representative modal analysis of some of the high pressure greyschists, not included in Okay [26], are given in table II. The jadeite + chloritoid paragenesis, common between Orhaneli and Keles (Fig. 5a), indicates metamorphic pressures of above 20 kbar, irrespective of the composition of the chloritoid.
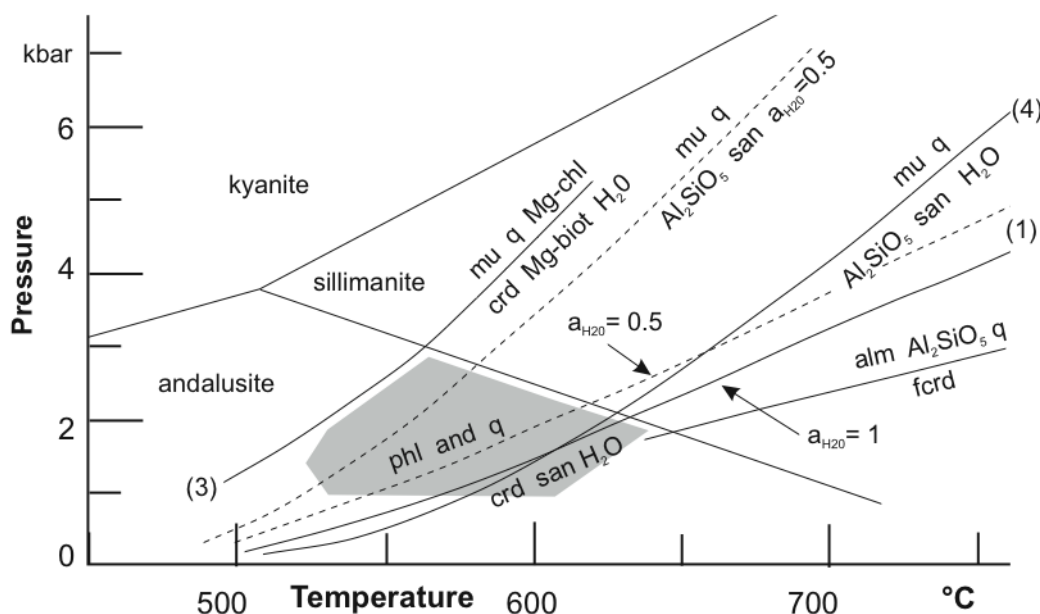
Figure 6: Pressure-temperature diagram showing the equilibria relevant for the estimation of the P-T conditions of the andalusite-cordierite schists from the Keles region. All reactions except (3) were calculated using THERMOCALC of Powell and Holland [28] and the thermodynamic data set of Holland and Powell [29]. The experimentally determined reaction (3) is after Seifert [69]. The P-T conditions of the Eocene metamorphism in the Uludağ area lie within the shaded region. Abbreviations: alm, almandine; and, andalusite; biot, biotite; chl,chlorite; crd, Mg-cordierite; fcrd, Fe-cordierite; m, muscovite; phl, phlogopite; q, quartz; san, sanidine.

Mineral equilibria in the greyschists in the Orhaneli-Keles area constrain tightly the peak P-T conditions during the metamorphism as 24 ± 3 kbar and $430 \pm 30°C$ [26].

Eastwards the high pressure minerals in the greyschists first disappear, then low pressure and high temperature minerals, such as biotite, andalusite and cordierite start to grow. The distance between the pristine blueschists with jadeite and chloritoid and the andalusite micaschists is about 15 km (Fig. 4). North of Keles, high pressure minerals, such as glaucophane and jadeite, are preserved only as pseudomorphs (Fig. 5b). In this region, the mineral assemblage in the greyschists is quartz + white mica + chlorite + chloritoid ± albite. Well preserved chlorite + albite + sericite pseudomorphs after glaucophane (Fig. 5) indicate that in this area metamorphic overprint of the blueschists involved no strain. Biotite in the greyschists appears within one kilometre of the Tepeldağ pluton. However, complete recrystallisation of the greyschists occurs in the schist band, two kilometre wide, between the two tongs of the Tepeldağ granitoid (Fig. 4). In this area the foliation in the schists, which is generally subhorizontal, is folded into a tight synform between the two granitoid bodies, and the greyschists are completely recrystallized into medium to coarse grained, finely banded, microfolded dark grey to black, andalusite-bearing gneissic schists. The common mineral assemblage in the andalusite micaschists is quartz + biotite + muscovite + andalusite + cordierite ± K-feldspar + graphite + ilmenite. In these micaschists quartz bands, a few millimetre thick, alternate with bands composed of biotite, feldspar, cordierite, andalusite and muscovite (Fig. 5c and d). The milimetre-scale banding overprints at a high angle the earlier foliation developed under the blueschist facies conditions. Cordierite is gener-

ally strongly pinitised and forms rounded grains, up to 2 mm across. Andalusite occurs as poikilitic porphyroblasts, up to 5 mm across, wrapped by biotite and muscovite. The formation of andalusite preceedes and overlaps the development of the new foliation. The early formed andalusite porphyroblasts are commonly bend (Fig. 5d) or strongly rotated (Fig. 5e), as shown by the spiral shaped graphitic inclusion trails. Andalusite continued to grow during the development of the new foliation, as indicated by the andalusite stringers emanating from the andalusite porphyroblasts and growing into the new fabric defined by the foliation (Fig. 5f).

Three andalusite-bearing gneissic schists are analysed with an SX-50 Cameca electron microprobe in the Bureau de Recherches Géologiques et Miniéres in Orléans, France. Operating conditions were 15 kV accelerating voltage, 12 nA beam current and 1 μm beam size. The estimated modes of the analysed specimens are given in table II, and representative mineral compositions in table III. The mineral assemblage in the schists is quartz + biotite + andalusite + cordierite + K-feldspar + plagioclase + muscovite + opaque. The plagioclase is oligoclase with anorthite contents of 14 to 24 %; the albite component in the K-feldspar is 9 to 13 %. The Fe/(Fe+Mg) ratios in biotite, muscovite and cordierite are 0.56-0.66, 0.45-0.53 and 0.46-0.47, respectively.

In the andalusite micaschist the metamorphic pressures are constrained by the reaction:

Biotite + andalusite + quartz = cordierite + K-feldspar + H$_2$O [1]
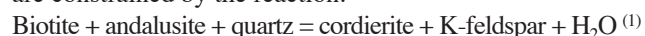
This reaction is shown in figure 6 for the mineral compositions in table III calculated using the THERMOCALC programme of Powell and Holland [28] and the thermodynamic data set of Holland and Powell [29]. The activities were determined using the AX program of T.J.B. Holland (wwww.esc.cam.ac.uk/astaff/holland).

**Table III:** Representative mineral compositions from the andalusite micaschists.

	4961						4966					5262				
	cord	and	biot	plag	K-felds	musc	and	K-felds	plag	biot	musc	and	biot	plag	musc	ilm
SiO2	48,02	37,98	35,79	60,30	64,77	46,43	37,58	64,90	64,44	35,88	46,12	37,14	35,88	63,50	46,65	3,63
TiO2	0,00	0,00	2,76	0,00	0,00	0,42	0,02	0,00	0,03	2,62	0,50	0,05	2,98	0,02	0,25	51,31
Al2O3	28,42	63,73	21,41	24,73	19,33	36,83	63,68	19,10	22,66	20,35	36,64	62,69	20,33	23,46	36,87	0,00
FeO	10,22	0,21	21,86	0,21	0,19	0,82	0,26	0,19	0,09	20,27	0,82	0,21	19,95	0,02	0,97	41,55
MgO	6,40	0,01	6,24	0,00	0,00	0,50	0,00	0,00	0,00	7,60	0,49	0,02	7,60	0,00	0,57	0,07
MnO	0,54	0,05	0,21	0,09	0,00	0,00	0,03	0,02	0,09	0,05	0,05	0,00	0,28	0,00	0,03	2,54
CaO	0,01	0,02	0,00	6,14	0,00	0,00	0,03	0,00	3,33	0,01	0,00	0,02	0,01	4,47	0,00	0,03
Na2O	0,24	0,01	0,19	7,82	1,20	0,59	0,02	0,96	9,57	0,20	0,65	0,03	0,19	8,66	0,51	0,00
K2O	0,01	0,03	8,71	0,13	14,92	10,49	0,00	14,58	0,32	9,46	10,32	0,02	9,36	0,22	10,59	0,00
Total	93,86	102,04	97,17	99,42	100,41	96,08	101,62	99,75	100,53	96,44	95,59	100,18	96,58	100,35	96,44	99,13
cations on the basis of																
	18oxy	5oxy	11oxy	8oxy	8oxy	11oxy	5oxy	8oxy	8oxy	11oxy	11oxy	5oxy	11oxy	8oxy	11oxy	3oxy
Si	5,24	2,01	2,68	2,70	2,97	3,05	2,00	2,98	2,83	2,70	3,05	2,00	2,69	2,79	3,06	0,18
Al	3,65	3,98	1,89	1,30	1,04	2,85	3,99	1,04	1,17	1,80	2,85	3,98	1,80	1,22	2,85	0,00
Ti	0,00	0,00	0,16	0,00	0,00	0,02	0,00	0,00	0,00	0,15	0,02	0,00	0,17	0,00	0,01	1,91
Fe2+	0,93	0,01	1,37	0,01	0,01	0,05	0,01	0,01	0,00	1,28	0,05	0,00	1,25	0,00	0,05	1,72
Mg	1,04	0,00	0,70	0,00	0,00	0,05	0,00	0,00	0,00	0,85	0,05	0,00	0,85	0,00	0,06	0,01
Mn	0,05	0,00	0,01	0,00	0,00	0,00	0,00	0,00	0,00	0,00	0,00	0,00	0,02	0,00	0,00	0,11
Ca	0,00	0,00	0,00	0,29	0,00	0,00	0,00	0,00	0,16	0,00	0,00	0,00	0,00	0,21	0,00	0,00
Na	0,05	0,00	0,03	0,68	0,11	0,08	0,00	0,09	0,82	0,03	0,08	0,00	0,03	0,74	0,07	0,00
K	0,00	0,00	0,83	0,01	0,87	0,88	0,00	0,86	0,02	0,91	0,87	0,00	0,90	0,01	0,89	0,00
Total	10,96	6,00	7,65	4,99	5,00	6,98	6,01	4,97	5,00	7,72	6,97	6,00	7,70	4,97	6,98	3,91
oxy, oxygens																

An important pressure sensitive reaction in low pressure metamorphism is:

muscovite + cordierite → andalusite + biotite + quartz + H_2O [2]

Pattison *et al.* [30] studied this reaction in detail and calculated a P-T grid calibrated for the Mg/(Mg+Fe) in biotite in equilibrium with muscovite, cordierite, andalusite and quartz. Using this grid the X_{Mg} value in the studied samples indicates a pressure of 1.5 kbar at 575°C.

Chlorite is singularly absent in the andalusite micaschists. An important reaction, which limits the high temperature stability of chlorite in metapelites in low pressure metamorphism is (Fig. 6):

Chlorite + muscovite + quartz = cordierite + biotite + H_2O [3]
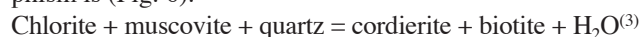
The stable coexistence of muscovite, quartz, andalusite and K-feldspar indicate that the P-T conditions are close to the reaction:

Muscovite + quartz = andalusite + K-feldspar + H_2O [4]

P_{H20} is generally regarded as being equal to the lithostatic pressure during metamorphism. However, in low pressure metamorphism (depths less than 10 km) P_{H20} can be less than lithostatic pressure because of fracture permeability of rocks at this depth [e.g., 31]. For a $X_{H20} = 0.5$, reactions (1) and (4) are only slightly displaced to lower temperatures and higher pressures (Fig. 6).

The presence of andalusite, and reactions (1), (2), (3) and (4) constrain metamorphic pressures to 2 ± 1 kbar and temperatures to 575 ± 50°C (Fig. 6) for the Eocene metamorphism in the Uludağ region. Absence of garnet is also compatible with metamorphism at very low pressures. Almandine garnet breaks down to cordierite at pressures of below 2 kbar in the andalusite stability field. Although addition of Mg will increase the stability of cordierite relative to garnet, in contact metamorphic aureoles garnet is apparently absent at pressures of less than 2 kbar and present at pressures above [32, p.159].

4.1. Contact or regional metamorphism?

The spatial association of the andalusite micaschists and the Tepeldağ granitoid, similar ages for the LP/HT metamorphism and granitoid emplacement (see below), and cordierite + andalusite paragenesis in the contact aureoles

of other granitoids in northwest Turkey may suggest that the andalusite micaschists south of Bursa are a product of contact rather than regional metamorphism. However, Eocene LP/HT metamorphism is clearly associated with progressive deformation involving the generation of new foliation and rotation of the andalusite porphyroblasts (Fig. 5d, e and f). Such deformation is not observed in the hornfels contact aureoles of the Orhaneli and Topuk granitoids. The Tepeldağ granitoid cuts the foliation in the andalusite micaschists, however, there is no evidence of contact metamorphism at the contact, indicating that the schists were already hot and deforming prior to the intrusion; the temperature was probably increased by the advection of heat into the upper crust by magmas. Intimate mixing of the contact and regional effects of the intrusions are also reported from several other regions [e.g., 33-35]. There is no difference between the P-T conditions of contact metamorphism and that
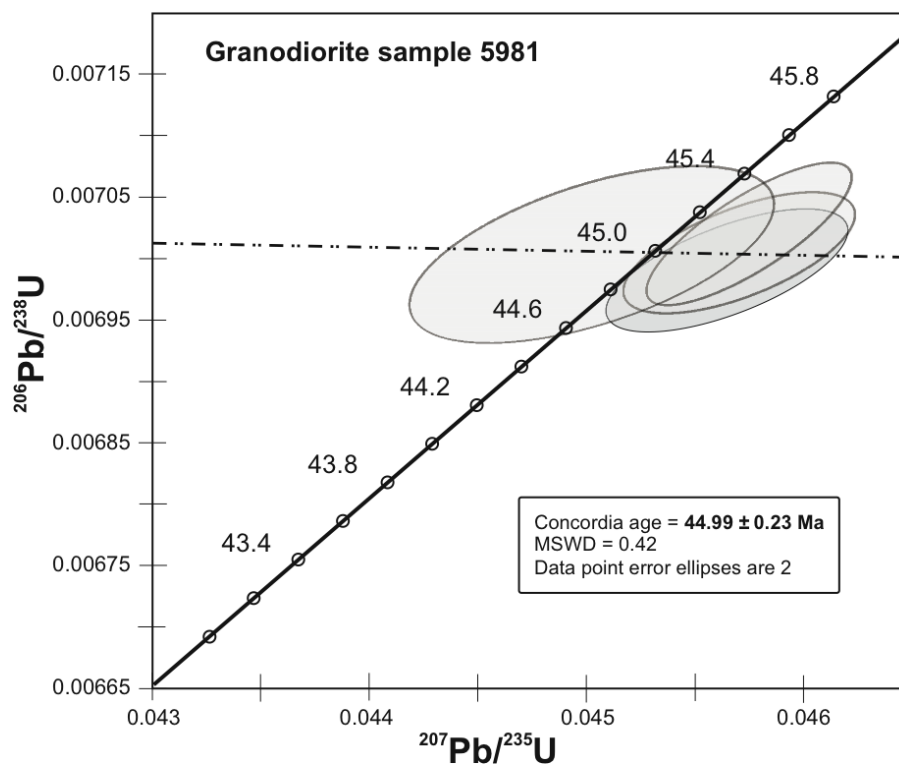

Figure 7: U-Pb Concordia diagram with four data points from abraded zircons (e. g., [70]) from the Tepeldağ pluton (sample 5981) that define a concordant age of about 45 ± 0.2 Ma (MSWD = mean square of weighted deviates).

of low pressure regional metamorphism [32, 36], and the two may only be separated by the absence or presence of an accompanying progressive ductile deformation.

5. Geochronology

Rb-Sr analyses were performed on biotite and muscovite from a micaschist (sample 5980) and on biotite from a sample (5981) from the Tepeldağ granitoid. Additionally U-Pb analyses were done on zircons from the Tepeldağ granitoid. The isotopic data are given in tables IV and V, and are shown in figure 7. The locations of the dated samples are marked on the geological map in figure 4

5.1. Methods

Mineral separation was performed by heavy liquids, magnetic separation and handpicking. For Rb-Sr dating, sample splits of about 50-100 mg were dissolved in Teflon breakers (perfluoralkoxy) with HF and $HClO_4$. For isotope analyses, Sr and light rare-earth elements were isolated on quartz columns by conventional ion exchange chromatography with a 5-ml resin bed of Bio Rad AG 50W-X12, 200-400 mesh. Sr was loaded with a Ta-HF activator on preconditioned W filaments and was measured in single-filament mode. The $^{87}Sr/^{86}Sr$ ratios were normalized to $^{86}Sr/^{88}Sr$=0.1194. The total procedure blank

for Sr and Rb is less than 0.5ng. Age determinations are based on the ^{87}Rb decay constant of 1.42×10^{-11} yr^{-1} as recommended by Steiger and Jaeger [37]. Isotope analyses were made on a Finnigan MAT 262 mass spectrometer in Tübingen. Analyses of Sr standarts National Bureau of Standarts NBS 987 gave $^{87}Sr/^{86}Sr$ ratios 0.710259±0.000010 (2 sigma of 28 analyses). The input error for age calculations are 1 % (2 sigma) for the $^{87}Rb/^{86}Sr$ ratios and 0.003 % (2 sigma) for the $^{87}Sr/^{86}Sr$ ratios. Regression lines were calculated by the least squares cubic method of York [38] using the ISOPLOT software of Ludwig [39] and Wendt [40]

U-Pb isotope analyses were performed on zircons. Zircons grains were separated from 200-63 ηm sieved rock fraction by standard separation techniques (milling, wet shaking table, magnetic and heavy liquid separation). Zircons were washed in 6N HCl then 7N HNO_3 spiked with a $^{205}Pb/^{235}U$ tracer solution, and dissolved in HF at 210ºC for 6 days in PTFE vessels in a Parr acid digestion bomb, as described by Parrish [41], using the vapour digestion method. Separation and purification of U and Pb was carried out in Teflon columns with a 40 –ul bed of AGI-X8 (100-200 mesh) and employing a HBr-HCl wash and elution procedure.

Pb was loaded with a mixture of Si gel and H_3PO_4 onto a single Re filament and measured at about 1300ºC. U was loaded with 1N HNO_3 and measured in a double Re- configuration mode. The thermal fractionation of Pb standard NBS 981

was measured, and the isotopic ratios corrected for 0.11 % fractionation per atomic mass unit. All measurements were performed with a Finnigan MAT 262 multicollector mass spectrometer operated in a static collection mode. Corrections for the remaining initial common Pb after the correction for tracer and blank were done using values from the Stacey and Kramers model [42]. Total procedural blanks for Pb and U were less than 10pg. More details on analytical techniques are given in Chen *et al.* [43] and Chen and Siebel [44]. The U-Pb data were evaluated with the Pbdat program [39]. Data were also treated without assumption for common Pb using the 3D model of Wendt [40]. Plots were made by use of Isoplot/Ex program version 2.06 [45].

5.2. Results

The sample dated from the Tepeldağ pluton is a monzo-diorite with plagioclase (54 %), K-feldspar (22 %), quartz (11 %), hornblende (17 %), biotite (5 %) and minor sphene, apatite and opaque. The biotite Rb-Sr age of this sample is 44.7 ± 0.4 Ma (table IV), which is indistinguishable from its U-Pb zircon age of 45.0 ± 0.23 Ma (table V, Fig. 7). This indicates intrusion and rapid cooling of the pluton in the Mid Eocene. The isotopic age of the Tepeldağ pluton is close to that of the Topuk granitoid (47.8 ± 0.4 Ma) [23], which shares a similar tectonic setting immediately south of the İzmir-Ankara suture.

The dated biotite-micaschist (5981) is a fine-grained rock with the mineral assemblage of quartz + plagioclase + biotite + muscovite + graphite (table II). Millimetric bands composed of biotite, plagioclase, muscovite and graphite alternate with bands of quartz. The length of the mica grains in the thin section is on the range 0.1-0.2 mm. The muscovite and biotite ages from the micaschist are 46.2 ± 2.7 and 39.1 ± 0.7, respectively (table IV). These ages are conformable with those from the Tepeldağ pluton, and with the field relations and indicate that the LP/HT metamorphism is temporally and genetically associated with the generation and emplacement of the Eocene plutons.

6. Tectonic evolution and origin of the Eocene thermal event

The region studied straddles a major Tethyan suture and its geology was shaped by the subduction, obduction, continental collision events in the Late Mesozoic and Tertiary, followed by the intrusion of the Eocene plutons and the associated LP/HT metamorphism. The earlier orogenic events are reviewed below in order to understand the cause of the Eocene magmatic-metamorphic episode.

Table IV: Rb-Sr isotopic data from the Uludağ region

Sample	Mineral	Rb, ppm	Sr, ppm	^{87}Rb/^{86}Sr	^{87}Sr/^{86}Sr	Age, Ma
biotite micaschist						
5980	rock	ww105.3	157.1	19,415	0,720396 ± 07	
	muscovite	164.9	46.65	10,248	0,725846 ± 10	**46.2 ± 2.7**
	biotite	397.5	21.27	54,296	0,750316 ± 09	**39.1 ± 0.7**
Tepelce granodiorite						
5981	rock	70.5	418.4	0.4876	0.706020 ± 10	
	biotite	432.8	2.1	623.06	1,101214 ± 14	**44.7 ± 0.4**

6.1. Subduction, obduction and continental collision

The northward subduction of the Neo-Tethyan oceanic lithosphere in the Turkish meridian started in the mid-Cretaceous and led to the development of a major accretionary complex [1, 2]. Radiolarian cherts in the extant accretionary complexes in western Turkey range in age from Late Triassic (Carnian) to mid Cretaceous indicating subduction of a Triassic to Cretaceous oceanic crust [21] . In contrast ophiolites in the western Turkey are of mid to late Cretaceous age (~93 Ma, Cenomanian) [22]. Their tectonic position above the accretionary complex and above the subducted continental crust suggests that they formed in a marginal basin above the Cretaceous subduction zone, in a similar manner envisaged for many of the Tethyan ophiolites [e.g., 46]. A supra-subduction zone origin for the northwest Turkey ophiolites is also compatible with their geochemistry, which involves a subduction zone signature [22].

The age and the estimated pressure of the HP/LT metamorphism in the Tavşanlı Zone show that by the Campanian (~80 Ma), the northern margin of the Anatolide-Tauride Block was subducted to a depth of at least 80 km (Fig. 8). This implies that oceanic subduction must have stopped by about the same time, which is in agreement with the termination of arc magmatism in the Pontides by the end of Campanian [47]. The net effect of continental subduction was the thrusting of a large slab of oceanic lithosphere southward over the Anatolide-Tauride Block. Remnants of this massive thrust sheet are found widely in the Taurides, where they usually rest on unmetamorphosed Mesozoic carbonates [e.g., 7, 48]. In the Anatolide-Tauride Block there is no clear break between the Campanian-Maastrichtian continental subduction - obduction event and the subsequent collision [47]. However, in the northern continent, on the southern margin of the Sakarya Zone, the Upper Cretaceous flysch to molasse sedimentation terminated by the Early Palaeocene and was followed by uplift, which may be taken as the time of the collision [2]. The sudden decrease in the convergence rate between Africa and Europe at 67 Ma [e.g., 49, 50] is probably related to the continental collision between the Anatolide-Tauride Block and the Europe (Fig. 8).

Early Palaeocene collision was coeval with uplift and widespread erosion in both the Sakarya Zone and in the northern margin of the Anatolide-Tauride Block. The next

Table V: U-Pb isotopic data from the Tepeldağ granodiorite, sample 5981

Zircon description	Sample weight in mg*	$^{206}Pb/^{204}Pb$	U (ppm)	Pb (ppm)	$^{208}Pb*/^{206}Pb*$	$^{206}Pb/^{238}U$	$^{207}Pb/^{235}U$	$^{207}Pb*/^{206}Pb*$
1 short prismatic	0.08	2373	1192	8.56	0.11007	0.00702 ± 05	0.04575 ± 39	0.04727 ± 24
2 thick prismatic	0.098	839.2	745.1	5.67	0.12735	0.00699 ± 04	0.04565 ± 45	0.04736 ± 36
3 thin xenomorphic	0.011	1924	5764	42.7	0.14468	0.00700 ± 04	0.04571 ± 44	0.04733 ± 34
3 short prismatic	0.011	2406	5612	42.4	0.14783	0.00700 ± 06	0.04502 ± 69	0.04664 ± 58

All errors quoted are 2σ absolute uncertainties and refer to the last digit   * = radiogenic ; grain size varies from 80-180μm

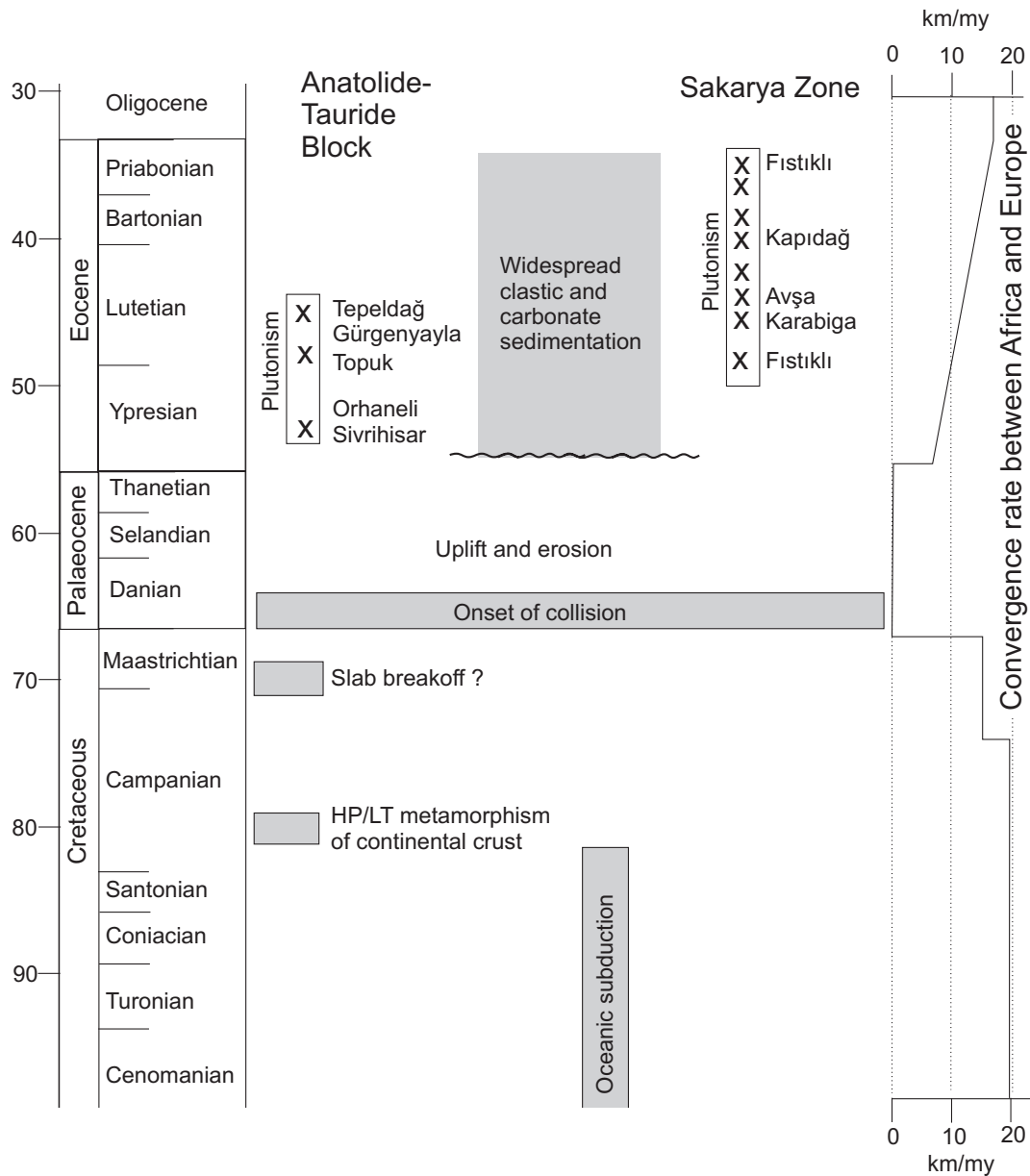mg* = error in weight is estimated to be up to 10%

Figure 8: Chronology of the tectonic events in northwest Turkey. The convergence rate between Africa and Europe is from Rosenbaum *et al.* [50] for a point in northern Africa at 24°E. The geological time scale is from Gradstein et al. [71]. For the source of other data see the text.

$^{206}Pb*/^{238}U$	$^{207}Pb*/^{235}U$	$^{207}Pb*/^{206}Pb*$
45.1	45.4	63.0
44.9	45.3	67.7
44.9	45.4	66.1
44.9	44.7	30.8

sedimentary depositional cycle in northwest Turkey started in the latest Palaeocene and Eocene; deposits of this age lie unconformable over a wide variety of metamorphic and sedimentary rocks (Fig. 3). Palaeocene-Eocene sedimentary rocks are not found in the Orhaneli area but crop out farther east in the Tavşanlı Zone, in the Tavşanlı and Eskişehir regions (Fig. 3) [51, 52]. In these areas Upper Palaeocene-Lower Eocene shallow marine limestones and shaly limestones lie unconformably over the accretionary complex or over the ophiolite. This suggests that Early Palaeocene uplift was rapidly replaced by subsidence in the Late Palaeocene and Early Eocene, when the crust was reduced to its normal thickness. The Eocene plutons were apparently emplaced in an extending region into a continental crust of normal crustal thickness.

6.2. Eocene magmatic-metamorphic event

Two possible causes for the post-collisional Eocene plutonism and associated LP/HT metamorphism are subduction of an oceanic lithosphere or slab breakoff. The strongest argument for subduction related magmatism during the Eocene are K-Ar and Rb-Sr age data from some of the other calc-alkaline plutons on the southern shores of the Marmara Sea (Fig. 3) [53]. The rather scattered biotite K-Ar cooling ages of these plutons range from Mid Eocene to latest Eocene (Karabiga 45.3 ± 0.9 Ma, southern Kapıdağ 38.2 ± 0.8 Ma and 36.1 ± 0.8 Ma, northern Kapıdağ 39.9 ± 0.8 Ma and 38.3 ± 0.8 Ma, Fıstıklı 48.2 ± 1.0 Ma and 35.4 ± 0.8 Ma). Rb-Sr biotite cooling ages from these granitoids also give a similar age range (southern Kapıdağ 35.0 ± 0.3 Ma, northern Kapıdağ 48.0 ± 0.5 Ma for the southern homogeneous part and 35.0 ± 0.3 Ma for the northern gneissic part, Avşa 44.0 ± 0.4 Ma, Satır *et al*. in preparation). Around the intrusions calcalkaline submarine volcanic rocks, mainly andesitic and dacitic lavas and pyroclastic rocks, are intercalated with Eocene marine sandstones [54]. The South Marmara plutonic belt, especially the Fıstıklı granitoid, is slightly offset with respect to the trend of the Tavşanlı intrusions (Fig. 3). However, if one compensates the poorly constrained but considerable (?50-100 km) dextral offset along the İzmir-Ankara suture [55], the South Marmara and Tavşanlı plutons form a linear magmatic belt, more than 400 km long and 60 km wide, extending in an WNE-ESE direction and straddling the İzmir-Ankara suture

(Fig. 3). The Eocene plutonic belt apparently does not extend into Greece; the granitoids in the Rhodope Massif are of Oligocene and younger age [56].

Oceanic subduction during the Eocene in the Eastern Mediterranean is indicated by the renewed start of convergence between Africa and Europe at 55 Ma (Fig. 8) [49, 50], by the tomographic studies [57] and by the paleogeographic reconstructions, which show an oceanic area, several hundred kilometres wide, to be subducted in the Eastern Mediterranean in the Eocene and later [e.g. 58]. The main problem with the subduction model is the location of the subduction zone. In modern subduction zones, the distance between the trench and the axis of the magmatic arc is 150-200 km [e.g., 59, p. 251], much less than the 700-750 km distance between the Eocene intrusions and the Hellenic trench. An oceanic subduction zone located farther north than the present Hellenic trench is an plausible alternative, especially as the Eocene HP/LT metamorphism in the Cyclades requires a subduction mechanism for its generation. The trend of the Eocene plutonic suite indicates a WNW-ESE trending subduction zone, subparallel to the Vardar suture. An Eocene oceanic subduction of a remnant oceanic lithosphere on the eastern part of the Vardar suture, north of the Pelagonian and Cycladic Massifs (Fig. 1) provides an explanation for the Eocene plutonic belt in northwest Turkey, as well as the Eocene HP/LT metamorphism in the Cyclades.

An alternative model for the Eocene magmatism in northwest Turkey is slab breakoff. The rupture of the oceanic lithosphere from the attached continental lithosphere, termed slab breakoff [60], has been invoked to explain, among others, the post-collisional granitoids in the Alps [61] and the late Caledonian granitoids in Britain [62]. Evidence favouring slab breakoff in northwest Turkey include:

a) restriction of the granitoids with well determined Ar-Ar, Rb-Sr and U-Pb Eocene ages to the Tavşanlı Zone, where continental subduction must have been followed by the rupture of the attached oceanic lithosphere,

b) the broadly linear pattern of the plutons aligned parallel to the İzmir-Ankara suture, compatible with a heat source limited in space and intensity,

c) the geochemical similarity between the Tavşanlı intrusions and the Ademello pluton in the Alps [23], regarded as a type example for the slab breakoff magmatism [61].

The pressure of blueschist facies metamorphism indicates that the slab breakoff occurred at a depth greater than 80 km. The uplift and exhumation of the HP/LT metamorphic rocks must have been aided by the slab breakoff, which removed a major force pulling the continental lithosphere down. Sodic amphibole detritus in the Maastrichtian sandstones in the Sakarya Zone [63] indicates that the blueschists were at least partly on the surface by that time. By the Late Palaeocene - Early Eocene the blueschists were on the surface in the eastern part of the Tavşanlı Zone and probably at a few kilometres depth in the western part. Therefore, slab breakoff probably occurred in the late Campanian or Maastrichtian (~70 Ma), which is the main period of exhumation of the blueschists.

This gives a period of 17 My between slab breakoff (70 Ma) and the start of Eocene plutonism (53 Ma) in northwest Turkey, in contrast with the inferred contemporaneous nature of slab breakoff and magmatism in the Alps [61]. However, the strongest argument against slab breakoff are the Eocene intrusions south of the Marmara Sea, which probably are linked genetically to those in the Tavşanlı Zone. Further geochemical and accurate age data from the South Marmara plutons will help to solve their relation to the Tavşanlı plutons.

7. Conclusions

A belt of Eocene intrusions, 400 km long and 60 km wide, extends in a WNW-ESE direction in northwest Turkey, straddling the İzmir-Ankara suture (Fig. 3). South of Bursa the plutons are associated with an Eocene LP/HT metamorphism developed in the Upper Cretaceous blueschists metapelites. A similar case of Eocene LP/HT metamorphism, possibly associated with an Eocene pluton, is reported from the Sivrihisar region [64, Whitney personal communication 2004]. Although the spatial association of the Eocene plutons with the Upper Cretaceous blueschists make slab breakoff an attractive mechanism for their genesis, the inferred 17 My age gap between slab breakoff and magmatism, and especially the extension of the plutonic belt 100 km northwest of the İzmir-Ankara suture (Fig. 3), makes this a less likely origin. Instead we suggest that the Eocene plutons and LP/HT metamorphism probably developed in a magmatic arc situated over a NNE dipping subduction zone located along the Vardar suture. This subduction zone was also responsible for the Eocene HP/LT metamorphism in the Cycladic Massif.

References

[1] Şengör, A.M.C., Yılmaz, Y., 1981. Tethyan evolution of Turkey: A plate tectonic approach. Tectonophysics, 75, 181-241.

[2] Okay, A.I., Tüysüz, O., 1999. Tethyan sutures of northern Turkey. In "The Mediterranean Basins: Tertiary extension within the Alpine orogen" (eds. B. Durand, L. Jolivet, F. Horváth and M. Séranne), Geological Society, London, Special Publication 156, 475-515.

[3] Sherlock, S., Kelley, S.P., Inger, S., Harris N., Okay, A.I., 1999. ^{40}Ar-^{39}Ar and Rb-Sr geochronology of high-pressure metamorphism and exhumation history of the Tavsanli Zone, NW Turkey. Contrib. Mineral. Petrol., 137, 46-58.

[4] Satir, M., Friedrichsen, H., 1986. The origin and evolution of the Menderes Massif, W-TRurkey: A rubidium/strontium and oxygen isotope study. Geol. Rundschau, 75, 703-714.

[5] Hetzel, R., Reischmann, T., 1996. Intrusion age of Pan-African augen gneisses in the southern Menderes Massif and the age of cooling after Alpine ductile extensional deformation. Geol. Mag., 133, 565-572.

[6] Bozkurt, E., Satır, M., 2000. The southern Menderes Massif (western Turkey): geochronology and exhumation history. Geol. J., 35, 285-296.

[7] Gutnic, M., Monod, O., Poisson, A., Dumont, J.F., 1979. Géologie des Taurides Occidentales (Turquie). Mémoires de la Sociéte Géologique de France, No. 137, 112 pp.

[8] Ketin, İ., 1947. Über die Tektonik des Uludağ-Massivs. Türkiye Jeoloji Kurumu Bülteni, 1, 75-88.

[9] Okay, A.I., Satır, M., 2000. Coeval plutonism and metamorphism in a latest Oligocene metamorphic core complex in northwest Turkey. Geol. Mag., 137, 495-516.

[10] Duru, M., Pehlivan, Ş., Şentürk, Y., Yavaş, F., Kar, H., 2004. New Results on the lithostratigraphy of the Kazdağ Massif in Northwest Turkey. Turk. J Earth Sci., 13, 177-186.

[11] Okay, A.I., Göncüoğlu, M.C., 2004. Karakaya Complex: a review of data and concepts. Turk. J. Earth Sci., 13, 77-95.

[12] Kaya, O., Mostler, H., 1992. A Middle Triassic age for low-grade greenschist facies metamorphic sequence in Bergama (Izmir), western Turkey: the first paleontological age assignment and structural-stratigraphic implications. Newsl. Strat., 26, 1-17.

[13] Okay, A.I., Altıner, D., 2004. Uppermost Triassic limestone in the Karakaya Complex - stratigraphic and tectonic significance. Turk. J. Earth Sci., 13, 187-199.

[14] Tekeli, O., 1981. Subduction complex of pre-Jurassic age, northern Anatolia, Turkey. Geology, 9, 68-72.

[15] Okay, A.I., 2000. Was the Late Triassic orogeny in Turkey caused by the collision of an oceanic plateau ? In: Bozkurt, E., Winchester, J.A., Piper, J.A.D. (Eds.) Tectonics and Magmatism in Turkey and Surrounding Area, Geological Society Special Publication, 173, pp. 25-41.

[16] Pickett, E.A., Robertson, A.H.F., 2004. Significance of the volcano-genic Nilüfer Unit and related components of the Triassic Karakaya Complex for Tethyan subduction/accretion processes in NW Turkey. Turk. J. Earth Sci., 13, 97-144.

[17] Altıner, D., Koçyiğit, A., Farinacci, A., Nicosia, U., Conti, M.A., 1991. Jurassic, Lower Cretaceous stratigraphy and paleogeographic evolution of the southern part of north-western Anatolia. Geol. Romana, 28: 13-80.

[18] Okay, A.I., 1984. Distribution and characteristics of the northwest Turkish blueschists. In: J.E. Dixon and A.H.F. Robertson (Editors), The Geological Evolution of the Eastern Mediterranean. Geol. Soc. London Spec. Publ., 17, 455-466.

[19] Lisenbee, A., 1971. The Orhaneli ultramafic-gabbro thrust sheet and its surroundings. A.S. Campbell (Editor), Geology and History of Turkey. Petroleum Exploration Society of Libya, Tripoli, pp. 349-360.

[20] Tankut, A., 1980. The Orhaneli Massif, Turkey. in: Panayiotou, A. (Ed.), Proceedings International Ophiolite Symposium, Cyprus 1979, pp. 702-713.

[21] Tekin, U.K., Göncüoğlu, M.C., Turhan, N., 2002. First evidence of Late Carnian radiolarians from the Izmir-Ankara suture complex, central Sakarya, Turkey: implications for the opening age of the Izmir-Ankara branch of Neo-Tethys. Geobios, 35, 127-135.

[22] Önen A.P., 2003. Neotethyan ophiolitic rocks of the Anatolides of NW Turkey and comparison with Tauride ophiolites. J. Geol. Soc. London, 160, 947-962.

[23] Harris, N.B.W., Kelley, S.P., Okay, A.I., 1994. Post-collision magmatism and tectonics in northwest Turkey. Contrib. Mineral. Petrol., 117: 241-252.

[24] Ataman, G., 1972. The radiometric age of the Orhaneli granodiorite (in Turkish). Türkiye Jeoloji Kurumu Bülteni, 15, 125-130.

[25] Ataman, G., 1973. The radiometric age of the Gürgenyayla (Domaniç) granodiorite (in Turkish). Türkiye Jeoloji Kurumu Bülteni, 16, 22-26.

[26] Okay, A.I., 2002. Jadeite-chloritoid-glaucophane-lawsonite schists from northwest Turkey: unusually high P/T ratios in continental crust. J. Metamorp. Geol., 20, 757-768.

[27] Okay A.I., Kelley, S.P, 1994. Tectonic setting, petrology and geochronology of jadeite + glaucophane and chloritoid + glaucophane schists from northwest Turkey. J. Metamorp. Geol., 12, 455-466.

[28] Powell, R., Holland, T.J.B., 1988. An internally consistent thermodynamic dataset with uncertainties and correlations: 3. Application methods, worked examples and a computer program. J. Metamorp. Geol., 6, 173-204.

[29] Holland, T.J.B., Powell, R., 1998. An internally consistent thermodynamic data set for phases of petrological interest. J. Metamorp. Geol., 16, 309-343.

[30] Pattison, D.R.M., Spear, F.S., Debuhr, C.L., Cheney, J.T., Guidotti, C.V., 2002. Thermodynamic modelling of the reaction muscovite + cordierite → Al2SiO5 + biotite + quartz + H_2O: constraints from natural assemblages and implications for the metapelitic petrogenetic grid. J. Metamorp. Geol., 20, 99-118.

[31] Norton, D., Knapp, R., 1977. Transport phenomena in hydrothermal systems: the nature of porosity. Am. J. Sci. 277, 913-936.

[32] Pattison, D.R.M., Tracy, R.J., 1991. Phase equilibria and thermobarometry of metapelites. In: Kerrick, D.M. (Ed.) Contact Metamorphism, Mineralogical Soceity of America, Reviews in Mineralogy, 26, pp. 105-207.

[33] Dickerson, R.P., Holdaway, M.J., 1989. Acadian metamorphism associated with the Lexington batholith, Bingham, Maine. Am. J. Sci., 289, 945-974.

[34] De Yoreo, J.J., Lux, D.R., Decker, E.R., Osberg, P.H., 1989. The Acadian thermal history of western Maine. J. Metamorph. Geol., 7, 169-190.

[35] Richards, S.W., Collins, W.J., 2002. The Cooma metamorphic complex, a low-P, high-T (LPHT) regional aureole beneath the Murrumbidgee Batholith. J. Metamorph. Geol., 20, 119-134.

[36] Miyashiro, A., 1973. Metamorphism and Metamorphic Belts. John Wiley and Sons, New York, 492 pp.

[37] Steiger, R.H., Jaeger, E., 1977. Subcommission on geochronology: Convention on the use of decay constants in geo- and cosmochronology. Earth Planet. Sci. Lett., 36, 359-362.

[38] York, D., 1969. Least-square fitting with a straight line with correlated errors. Earth Planet. Sci. Lett., 5, 320-324.

[39] Ludwig, K.R., 1988. A plotting and regression program for radiogenic-isotope data for IBM-PC compatible computers, U.S. Geol. Surv. Open File Rep., 88-557, 1-16.

[40] Wendt, I., 1984. A three dimensional U-Pb discordia plane to evaluate samples with common lead of unknow isotopic composition. Isot. Geosci. 2, 1-12.

[41] Parrish, R. R., 1987. An improved micro-capsule for zircon dissolution in U-Pb geochronology. Chem. Geol 66: 99-102.

[42] Stacey, J. S., Kramers, J. K., 1975. Approximation of terrestrial lead isotope evolution by a two-stage model. Earth Planet. Sci. Lett. 26, 207-221.

[43] Chen, F., Siebel, W., Satir, M., Terzioglu, N., Saka, K., 2002. Geochronology of the Karadere basement (NW Turkey) and implications for the geological evolution of the Istanbul zone. Int. J. Earth Sci.,91, 469-481.

[44] Chen, F., W. Siebel, 2004. Zircon and titanite geochronology of the Fürstenstein granite massif, Bavarian Forest, NW Bohemian Massif: Pulses of the late Variscan magmatic activity. Eur. J. Mineral. 16, 777-788.

[45] Ludwig, K. R., 1999. Isoplot/Ex, version 2.06: a geochronological tool-kit for Microsoft Excel. Berkeley Geochronology Center Spec. Pub. 1a, 1-49.

[46] Robertson, A.H.F., 2002. Overview of the genesis and emplacement of Mesozoic ophiolites in the Eastern Mediterranean Tethyan region. Lithos, 65, 1-67.

[47] Okay A.I., Tansel, İ., Tüysüz, O., 2001. Obduction, subduction and collision as reflected in the Upper Cretaceous-Lower Eocene sedimentary record of western Turkey. Geol. Mag., 138, 117-142.

[48] Dilek, Y., Thy, P., Hacker, B., Grundvig, S., 1999. Structure and petrology of Tauride ophiolites and mafic dike intrusions (Turkey): Implications for the Neotethyan ocean. Geol. Soc. Am. Bull., 111, 1192-1216.

[49] Dewey, J.F., Helman, M.L., Turco, E., Hutton, D.H.W., Knott, S.D. 1989. Kinematics of the western Mediterranean. In: Coward, M.P., Dietrich, D., Park, R.G. (eds), Alpine Tectonics, Geological Society Special Publication 45, 265-283.

[50] Rosenbaum, G., Lister, G.S., Duboz, C. 2002. Relative motions of Africa, Iberia and Europe during Alpine orogeny. Tectonophysics, 359, 117-129.

[51] Baş, H., 1986. Tertiary geology of the Domanic-Tavşanlı-Kütahya-Gediz region (in Turkish). Jeoloji Mühendisliği, 27,11-18.

[52] Karabaşoğlu, A., Erdem, N.Ö., Akyazı, M., 2002. Foraminiferal biostratigraphy of the Palaeocene/Eocene units south of Eskişehir. Abstracts of the 55. Geological Congress of Turkey, Ankara, p. 141-142.

[53] Delaloye, M., Bingöl, E., 2000. Granitoids from western and northwestern Anatolia: geochemistry and modelling of geodynamic evolution. Int. Geol. Rev., 42, 241-268.

[54] Siyako, M., Bürkan, K.A., Okay, A.I., 1989. Tertiary geology and hydrocarbon potential of the Biga and Gelibolu peninsulas (in Turkish). Bulletin of the Turkish Association of Petroleum Geologists, 1, 183-199.

[55] Okay, A.I., Harris, N.B.W., Kelley, S.P., 1998. Exhumation of blueschists along a Tethyan suture in northwest Turkey. Tectonophysics, 285, 275-299.

[56] Baltatzis, E., Esson, J., Mitropoulos, P., 1992. Geochemical characteristics and petrogenesis of the main granitic intrusions of Greece: an application of trace element discrimination diagrams. Mineral. Mag., 56, 487-501.

[57] Spakman, W., Wortel, M.J.R., Vlaar, N.J., 1988. The Hellenic sub-duction zone: a tomographic image and its geodynamic implications. Geophys. Res. Lett., 15, 60-63.

[58] Smith, A.G., Hurley, A.M., and Briden, J.C., 1981. Phanerozoic paleocontinental world maps. Cambridge University Press, 102 pp.

[59] Windley, B.F. 1986. The Evolving Continents. Second edition, John Wiley & Sons Ltd., 399 pp.

[60] Davies JH, von Blanckenburg F., 1995. Slab breakoff - a model of lithosphere detachment and its test in the magmatism and deformation of collisional orogens. Earth Planet. Sci. Lett. 129, 85-102, 1995

[61] von Blanckenburg F, Davies JH, 1995. Slab breakoff - a model for syncollisional magmatism and tectonics in the Alps. Tectonics, 14, 120-131.

[62] Atherton M.P., Ghani A.A., 2002. Slab breakoff: a model for Caledonian, Late Granite syn-collisional magmatism in the orthotectonic (metamorphic) zone of Scotland and Donegal, Ireland. Lithos, 62, 65-85.

[63] Batman, B., 1978. Geological evolution of the region north of Haymana and the study of the melange in the region (in Turkish). Yerbilimleri, 4, 95-124.

[64] Whitney, D.L., 2002. Coexisting andalusite, kyanite, and sillimanite: Sequential formation of three Al_2SiO_5 polymorphs during progressive metamorphism near the triple point, Sivrihisar, Turkey. Am Mineral. 87, 405-416.

[65] Okay, A.I., Satır, M., Tüysüz, O., Akyüz, S., Chen, F., 2001. The tectonics of the Strandja Massif: Variscan and mid-Mesozoic deformation and metamorphism in the northern Aegean. Int. J. Earth Sci., 90, 217-233.

[66] Konak, N., 2002. Geological map of Turkey, İzmir sheet, 1. 500 000. Maden Tetkik ve Arama Genel Müdürlüğü, Ankara.

[67] Türkecan, A., Yurtsever, A., 2002. Geological map of Turkey, Istanbul sheet, 1. 500 000. Maden Tetkik ve Arama Genel Müdürlüğü, Ankara.

[68] Can, A., 1961. Petrographische und Lagerstattenkundliche Untersuchungen in südlichen Teil des Granitmassives vom Uludağ bei Bursa, Türkei. Ph.D. thesis, University of Bonn, 77 pp.

[69] Seifert, F., 1970. Low-temperature compatibility relations of cordierite in haplopelites of the system K_2O-MgO-Al_2O_3-SiO_2-H_2O. J. Petrol, 11, 73-99.

[70] Krogh, T. E., 1982. Improved accuracy of U-Pb zircon agesby the creation of more concordant systems using an air abrasion technique. Geochim. Cosmochim. Acta 46, 673-649.

[71] Gradstein, F.M., Ogg, J.G., Smith, A.G., Bleeker, W, Lourens, L.J., 2004. A new geological time scale with special reference to Precambrian and Neogene. Episodes, 27, 83-100.